Polymer Journal (2018) 50:989–996
https://doi.org/10.1038/s41428-018-0084-0

ORIGINAL ARTICLE

Binding sites and structure of peptides bound to SiO_2 nanoparticles studied by solution NMR spectroscopy

Yu Suzuki[1] · Heisaburo Shindo[2]

Received: 23 January 2018 / Revised: 23 April 2018 / Accepted: 23 April 2018 / Published online: 7 June 2018

Abstract

Understanding the mechanism of the interaction between inorganic materials and peptides is important for the development of organic/inorganic hybrid materials. The titanium-binding peptide (TBP; Arg1-Lys2-Leu3-Pro4-Asp5-Ala6) has been reported to possess a high binding affinity to SiO_2 as well as TiO_2 surfaces. Here, we report the binding modes and mechanism of the TBP to SiO_2 nanoparticles. To accomplish this objective, we analyzed the binding sites of the TBP to a SiO_2 surface and the structure of the TBP bound to the SiO_2 using solution NMR spectroscopy. Saturation transfer difference (STD) NMR analysis was performed to identify the TBP sites that interact with the SiO_2 surface, and then Arg1 and Asp5 were identified to be in close contact with the SiO_2 surface. The structure of the TBP bound to SiO_2 was well defined, and the Arg1 and Asp5 side chains face in the same direction. The combination of these results validates that the guanidyl group of Arg1 and the carboxyl group of Asp5 interact electrostatically with the silanol groups SiO^- and $SiOH_2^+$ on the SiO_2 surface, respectively. The binding mode of TBP/SiO_2 was found to be different from that of the TBP/TiO_2 system, which has been previously reported.

Introduction

The nanoscale engineering of organic/inorganic hybrid materials continues to grow. The adhesion and selectivity at the interface of biomacromolecules and inorganic materials are critical to the construction of well-organized hybrid materials. To address this point, peptide motifs that interact with inorganic materials have specifically been used [1, 2]. Peptides with a specific binding affinity towards inorganic materials have been used to prepare nanostructured materials with novel properties and functions, such as surface biocompatibility, drug delivery and the construction of nanodevices [3–5].

A common approach to identify binding peptides for a target material is the use of combinatorial phage display libraries [3, 6, 7]. By this approach, a large number of the peptides binding to a wide range of materials are isolated, and a large collection of material binding peptides is available. Several peptides with significantly different amino acid sequences have been identified for certain materials such as silica, titania, and gold [2]. The reason for the propensity of such peptides with different sequences is still unclear although many approaches have been employed to assess the affinity of peptides for targeted inorganic surfaces.

The interactions between peptides and the surfaces of inorganic materials are affected by several parameters related to both the properties of the peptide and the material surface, i.e., the structure, conformation and flexibility of the peptide backbone and the topography, roughness and chemical nature of the surface. Recently, it was reported that the particle size and pH in the solution largely influence peptide adsorption on silica nanoparticle surfaces [8–11]. These studies showed that peptide adsorption increased with increasing particle size due to the increased surface charge associated with the particle size [9]. In addition, higher pH values in the solution resulted in a higher negative charge density on the silica surface and shifted the adsorption toward the positively charged peptides [10]. Therefore, it is advantageous to assess the binding

✉ Yu Suzuki
suzukiyu@u-fukui.ac.jp

[1] Tenure-Track Program for Innovative Research, University of Fukui, 3-9-1, Bunkyo, Fukui-shi, Fukui 910-8507, Japan

[2] School of Pharmacy, Tokyo University of Pharmacy and Life Sciences, 1432-1, Horinouchi, Hachioji, Tokyo 192-0392, Japan

mechanism of a certain peptide to the distinct inorganic material under comparable sample conditions such as the particle size, pH and salt concentration in the solution for understanding the specific binding affinity of the peptides.

The titanium-binding peptide (TBP) is one of artificially selected peptides by phage display method with a length of six amino acids (Arg1-Lys2-Leu3-Pro4-Asp5-Ala6); this peptide binds to the surface of metal oxides with high selectivity [12, 13]. The TBP has subsequently been used in nanobiotechnological applications such as functionalizing the surfaces of medical titanium materials [14–16] and multilayer constructions using its binding and mineralization properties [17, 18]. Characterization studies of the TBP have revealed that it is bound to the oxide surfaces of both silicon as well as titanium in aqueous solution [12, 19].

Saturation transfer difference (STD) experiments [20–22] had been developed to identify or characterize the ligands that bind to the large protein when the protein is saturated by strong irradiation and the magnetization transfer from the protein to ligand molecules is observed. In a previous study, we have reported solution NMR studies of the interactions between the TBP and TiO_2 nanoparticle surfaces [23]. We showed that STD technique is a powerful tool to identify the binding sites of the peptides bound to the TiO_2 nanoparticles suspended in an aqueous solution. Water molecules were selectively saturated by strong irradiation, and the magnetization transfer from the saturated water protons to the TiO_2-bound peptides was measured.

In this study, we investigated the binding sites and structure of the TBP bound to SiO_2 nanoparticles, and the results were compared with the case of TiO_2 nanoparticles. First, we measured the relaxation time $T_{1\rho}$ to evaluate the dynamic nature of the TBP interacting with the SiO_2 surface. Second, we conducted STD NMR measurements to identify the TBP sites that interact with the SiO_2 surface. Third, we performed mutagenesis experiments to elucidate the roles of the individual residues of the TBP in its interaction with SiO_2 nanoparticles. Fourth, we conducted NOESY experiments to determine the three-dimensional structure of the TBP bound to the SiO_2 surface. Finally, on the basis of these NMR results combined with the surface potential of the SiO_2 nanoparticles, we proposed a model for the binding of the TBP onto the SiO_2 surface and discussed the TBP binding mechanisms for the two different nanoparticles, SiO_2 and TiO_2.

Materials and methods

Sample preparation

Peptides with a purity greater than 98% were purchased from Funakoshi Co., Ltd., Japan. The amino acid sequence of the TBP is Arg-Lys-Leu-Pro-Asp-Ala (RKLPDA), whereas those of the analogues are AKLPDA (R1A), RALPDA (K2A), RKLADA (P4A), and RKLPAA (D5A); the abbreviations used in this study for these peptides are shown in parentheses. SiO_2 nanoparticles with particle sizes ranging from 10 to 20 nm were purchased from Sigma-Aldrich, USA.

The SiO_2 nanoparticles were suspended in water and sonicated twice for 10 min by using a 50% duty cycle. The nanoparticle suspension was then mixed with the peptide solution, and the pH of the resulting suspension was adjusted to 7.0. The final concentrations of the nanoparticles and peptides were 1 mg/mL and 6 mM, respectively, in a 20 mM phosphate buffer (pH 7.0) containing 10% D_2O.

NMR measurements

NMR measurements were performed on ECA600II (JEOL, Japan) operating at a ^1H frequency of 600.17 MHz at 298 K. Resonance assignments for the ^1H signals were completed in a previous study [23]. The T_1 and $T_{1\rho}$ relaxation times were measured by the inversion recovery method and the spin-lock method, respectively. The times for the T_1 measurements were set to 10, 50, 100, 200, 300, 400, 500, 700, 1000, 3000, and 5000 ms, and the spin-lock times for the $T_{1\rho}$ measurements were set to 5, 10, 20, 30, 40, 50, 60, 80, 100, 150, 200, 500, and 1000 ms.

STD NMR was used to identify the segments of the peptides that are in close contact with the SiO_2 surface. The selective saturation was composed of a sequence of Gaussian-shaped pulses with saturation lengths of 60 ms and an attenuation of 71.5 dB. The number of selective pulses ranged from 10 to 160, leading to total lengths of 0.6–9.6 s for the saturation pulse sequences to obtain the STD buildup curves. The on-resonance irradiation of water molecules was performed at a chemical shift of 4.7 ppm, and off-resonance irradiation was applied at −10 ppm. The number of scans acquired for one-dimensional STD NMR was 256. The NMR data were processed using the Delta program on the ECA600II instrument.

The ^1H-^1H TOCSY and ^1H-^1H NOESY measurements of the TBP/SiO_2 mixtures were measured to determine the three-dimensional structure of the TBP bound to SiO_2. TOCSY spectra were recorded using an MLEV-17 mixing sequence employing a mixing time of 50 ms, a spectral width of 15 ppm in both the t_1 and t_2 dimensions, and 256 and 1024 complex points in the t_1 and t_2 dimensions, respectively. NOESY spectra were recorded with a mixing time of 150 ms, a spectral width of 15 ppm in both the t_1 and t_2 dimensions, and 256 and 1024 complex points in the t_1 and t_2 dimensions, respectively. The NMR data were processed using NMRPipe [24], and the two-dimensional spectra were analyzed using SPARKY [25]. The distance constraints obtained were input into the DYANA [26] program to determine the three-dimensional structure.

Analysis of the STD data

The STD factor A_{std} is defined as $A_{std} = (I_0 - I_{sat})/I_0$, where I_0 is the intensity of a given signal in the off-resonance or reference NMR spectrum, I_{sat} is the intensity of a signal in the on-resonance NMR spectrum, and $(I_0 - I_{sat})$ represents the intensity of the STD spectrum [21, 27]. Thus, A_{std} represents the intensity of a saturated spectrum as a fraction of the intensity of an unsaturated reference spectrum. To eliminate the T_1 bias at long saturation times, we calculated the slope of the STD buildup curve at saturation time zero by fitting the saturation curve by using $A_{std} = A_{max}(1 - \exp(-k_{sat} \cdot t_{sat}))$, where A_{std} is the STD factor of a given proton at saturation time t_{sat}, A_{max} is the maximal STD factor when long saturation times are used, and k_{sat} is the saturation rate constant [20]. The multiplication of k_{sat} by A_{max} yields the initial slope of the buildup curve at zero saturation time, which corresponds to the STD intensity without the T_1 bias; this is denoted as STD_0.

Results and discussion

Relaxation rates of the TBP bound to SiO_2

^{1}H NMR spectrum and the signal assignments of the TBP/SiO_2 sample in aqueous solution at pH 7 are shown in Fig. 1a. To evaluate the dynamic nature of the TBP bound to the surface of SiO_2 nanoparticles, the relaxation times T_1 and $T_{1\rho}$ of the Hβ protons of the individual residues in the TBP were measured in the presence and absence of the SiO_2 nanoparticles, respectively. The reciprocals of T_1 and $T_{1\rho}$, i.e., the relaxation rates R_1 and $R_{1\rho}$, respectively, are plotted in Fig. 2. The relaxation rates of the Hβ protons for each residue (except for Leu3, in which the Hδ proton was used because of the peak overlap of Leu3 Hβ with the other peaks) are plotted in the order of the residue number. The observed relaxation rates are the weighted average of the rates of the TBP bound to SiO_2 and the free TBP in solution. The R_1 values of the bound TBP are very small because of the extremely slow motion limit of the SiO_2 nanoparticles, and thus, the observed R_1 values are in fact those of the free TBP. On the other hand, the $T_{1\rho}$ values of the bound TBP are very short because of the extremely slow motion limit of the SiO_2 nanoparticles, and therefore, the observed $R_{1\rho}$ values depend on the fraction of the bound TBP and its mobility. As expected, the R_1 values of each residue are approximately the same between the TBP alone and the TBP in the presence of SiO_2. This similarity is because the amount of TBP bound to the SiO_2 surface is considerably smaller in the fraction than in the bulk, and the TBP/SiO_2 has very small R_1 values. In contrast, the $R_{1\rho}$ values for TBP/SiO_2 are higher than those of TBP alone, indicating that the TBP in the bound state substantially

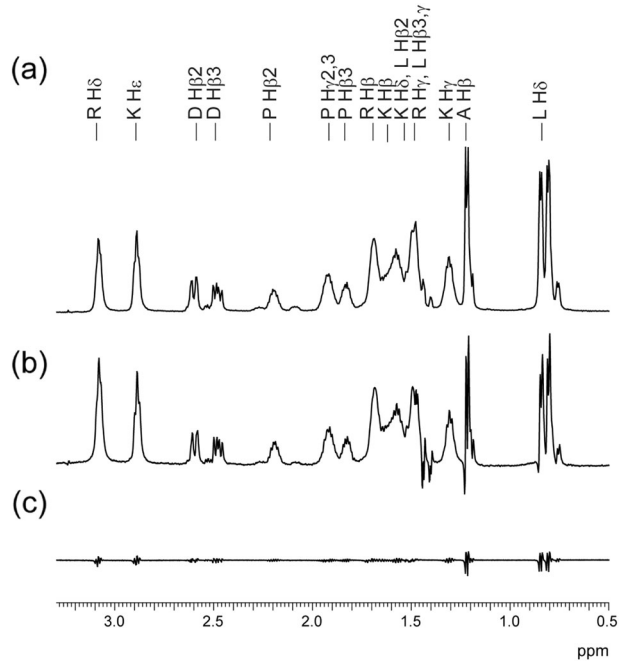

Fig. 1 **a** 1D ^{1}H NMR spectrum of the TBP/SiO_2 sample in solution and their signal assignments; **b** 1D STD NMR spectrum of the TBP in the TBP/SiO_2 sample; and **c** 1D STD NMR spectrum of the TBP alone in solution

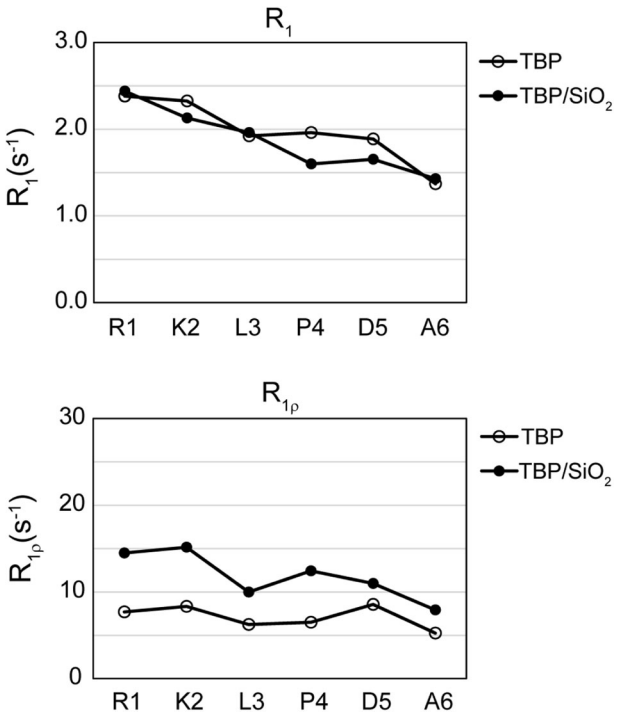

Fig. 2 Relaxation rate (R_1 and $R_{1\rho}$) plots of Hβ for each residue in the TBP in the absence of SiO_2 (○) and in the presence of SiO_2 (●)

contributes to the observed $R_{1\rho}$ despite its small fraction relative to that of the free TBP in solution. Thus, it is confirmed that the TBP has a binding affinity to the SiO_2 nanoparticles.

Binding sites of the TBP to SiO_2 as identified by the STD

STD NMR measurements were performed to identify the TBP residues that interact with the SiO_2 surface. In this study, water molecules were selectively saturated by strong irradiation at 4.7 ppm, which corresponds to the water peak, and a difference spectrum between the on-resonance saturation at the water peak and the off-resonance saturation at −10 ppm was recorded. The details of the STD measurement and its mechanism are reported in our previous article [23]. 1D STD spectra for the TBP/SiO_2 sample and TBP alone are shown in Fig. 1b, c. The STD peaks were only observed in the presence of SiO_2 (Fig. 1b) but not observed in the absence of SiO_2 (Fig. 1c). These results provide clear evidence for the occurrence of the saturation transfer from water molecules to the TBP molecules bound to the SiO_2 surface and the fast exchange between the bound and free TBPs.

The STD amplification factor (A_{std}) values for well-separated peaks are plotted against saturation time in Fig. 3. A_{std} is obtained from the peak intensity in the STD spectrum divided by the peak intensity in the 1D ^1H spectrum (Fig. 1a). A_{std} for Arg1 Hδ is the largest among the protons measured, followed by Lys2 Hε. To evaluate the STD factor more quantitatively, the initial slope of the STD buildup curve was calculated by fitting the saturation curve. The initial slope of the buildup curve at a zero saturation time is denoted as STD_0. The calculated A_{max}, K_{sat}, and STD_0 values for well-separated protons are listed in Table 1.

To compare the STD_0 values of the Hβ protons (Hδ proton for Leu3) of the residues, the largest STD_0 value, i.e., that for Arg1 Hβ, was set to 100%. The relative STD_0 values in % for each residue are represented using the bar graph in Fig. 4. The black bars represent the STD_0 values for TBP/SiO_2. Lys2 Hβ has the second largest relative STD_0 value (89%), followed by Asp5 Hβ (64%). Leu3 Hδ and Pro4 Hβ have similar relative STD_0 values (53 and 56%, respectively). The lowest relative STD_0 is 33% for Ala6 Hβ at the C-terminal residue. This result indicates that Arg1 and Lys2 are in the closest contact with the SiO_2 surface and that Leu3-Asp5 is also relatively close to the surface. Compared to the previously reported STD_0 values of the TBP/TiO_2 sample (white bars), the STD_0 values of Leu3-Asp5 are much smaller than those of the TBP/SiO_2 sample, whereas the STD_0 of the N-terminal residues Arg1 and Lys2 are nearly 100% for both TBP/SiO_2 and TBP/TiO_2. This difference between the TBP/SiO_2 and TBP/TiO_2 samples suggest that Leu3-Asp5 and most likely Asp5 play the key role as well as the N-terminal residues for binding to the SiO_2 surface.

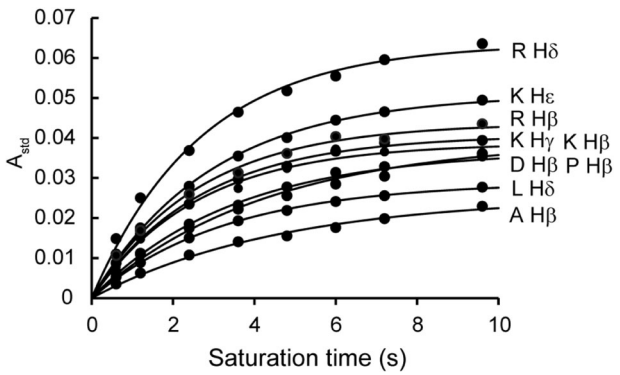

Fig. 3 STD amplification factors plotted against the saturation time for the well-separated peaks

Table 1 STD parameters of the TBP sample in the presence of SiO_2 nanoparticles

Residue	Observed protons	A_{max}	$K_{sat}(s^{-1})$	STD_0 ($\times 10^{-2}s^{-1}$)
Arg1	Hβ	0.044	0.38	1.67
Arg1	Hδ	0.064	0.37	2.38
Lys2	Hβ	0.039	0.38	1.49
Lys2	Hγ	0.041	0.38	1.53
Lys2	Hε	0.051	0.34	1.72
Leu3	Hδ	0.029	0.30	0.88
Pro4	Hβ	0.040	0.23	0.93
Asp5	Hβ	0.037	0.29	1.06
Ala6	Hβ	0.025	0.21	0.55

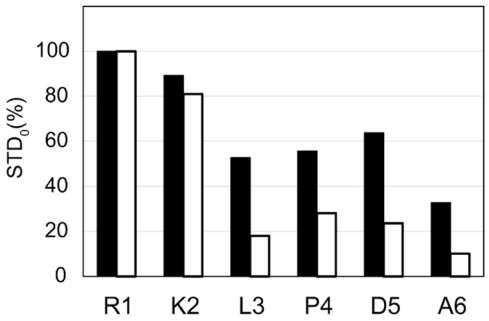

Fig. 4 Bar graph of the relative initial rate of the A_{std} buildup curve, STD_0, for the Hβ protons of each residue (except L3 Hδ). The STD_0 value for the Hβ proton of R1 is set to 100%. The black bars represent the TBP/SiO_2 sample obtained in this study, and the white bars represent the TBP/TiO_2 sample reported previously for comparison

STD of the TBP analogues

As described above, STD measurements showed that not only the N-terminal residues but also the Asp5 residue play

(a)

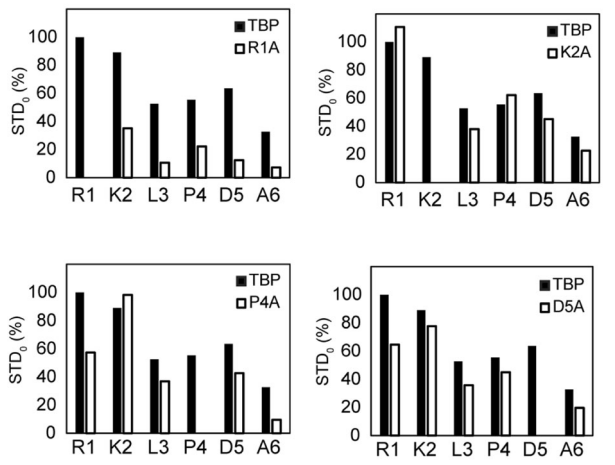

(b)

	R1A	K2A	P4A	D5A
SiO_2	↓↓	→	↓	↓
TiO_2	precipitate	precipitate	↓	↑

Fig. 5 **a** Bar graph of the relative STD_0 values for the Hβ protons of each residue along the TBP chain (except L3 Hδ) (black bars) and for the TBP analogues R1A, K2A, P4A, and D5A (white bars). Here, the STD_0 values for the Hβ protons of R1 of TBP are set to 100%. **b** The results of the TBP analogue experiments for TBP/SiO_2 obtained in this study and those for TBP/TiO_2 reported previously are summarized

key roles in the interaction between TBP and the SiO_2 nanoparticles. To confirm the above, we performed a site-directed mutation analysis by alanine replacements; **A**KLPDA (R1A), R**A**LPDA (K2A), RKL**A**DA (P4A), and RKLP**A**A (D5A). All these TBP analogues maintained the suspended form of SiO_2 nanoparticles, whereas the TiO_2 nanoparticles suspended in an aqueous solution precipitated in the presence of R1A and K2A, as shown in the previous study (See also Fig. 5b). The binding abilities of R1A, K2A, P4A, and D5A with the SiO_2 surface were evaluated by STD measurements. STD buildup curves were obtained for each analogue, and the value of STD_0 was calculated from the initial slopes. The STD_0 values for the TBP analogues and those of the native TBP are represented by bar graphs in Fig. 5a. The STD_0 values for R1A are significantly smaller for all residues than those for the intact TBP, indicating that Arg1 is the crucial residue for the interaction between the TBP and SiO_2 surfaces, as observed for the TBP/TiO_2 system. Interestingly, the effect of the replacement of Lys with Ala on STD_0 is insignificant for all residues, indicating that the Lys residue is not directly involved in the interaction with the SiO_2 surface. The spatial proximity of Lys2 to Arg1, which has the strongest interaction with the SiO_2 surface, is likely a part of the origin for it having the second largest STD_0 value. The STD_0 values of residues Arg1, Leu3, Asp5, and Ala6 of P4A are smaller than those of the intact TBP. Particularly, the STD_0 values of the terminal residues Arg1 and Ala6 in P4A are <60% of those observed for the corresponding residues in the intact TBP, suggesting that the conformational rigidity due to Pro4 is important for TBP binding to SiO_2.

D5A exhibits a low STD_0 at all residues, e.g., the STD_0 at Arg1 decreases to nearly 60% relative to that of the intact TBP. This result is very interesting because the STD_0 values increased at all residues for the D5A/TiO_2 sample, as reported in a previous study [23]. The mutation of Asp to Ala provided a different effect between SiO_2 and TiO_2, suggesting that the negatively charged COO^- group of Asp5 interacts electrostatically with a positively charged protonated silanol group, $SiOH_2^+$, on the SiO_2 surface.

The results of the TBP analogue experiments for TBP/SiO_2 obtained in this study and those for TBP/TiO_2 reported previously are summarized in Fig. 5b. The TBP mutation study reveals that Asp5 as well as Arg1 plays a key role in the interactions with SiO_2 nanoparticles, whereas Arg1 and Lys2 have a key role in the interaction with TiO_2 nanoparticles. These results strongly suggest that the binding mode or/and structure of the TBP are different between the SiO_2 and TiO_2 nanoparticles.

Comparison of the STD_0 at different pH values

The TBP mutation study suggested that an electrostatic interaction exists between the COO^- group of Asp5 and the SiO_2 surface. To confirm this point, the STD measurements of a TBP/SiO_2 sample at different pH values of 7 and 9 were performed. The relative STD_0 values of the TBP at pH 7 and 9 are represented by the bar graph in Fig. 6. The values of STD_0 at pH 9 are smaller for all residues except for Arg1 than those for the corresponding residues at pH 7. The STD_0 values for Lys2 and Pro4 decrease to nearly 70%, and those for Leu3, Asp5, and Ala6 decrease to nearly 40%. The zeta potentials of an aqueous SiO_2 dispersion were measured, and the values were −26 mV at pH 7 and −40 mV at pH 9. A reduced

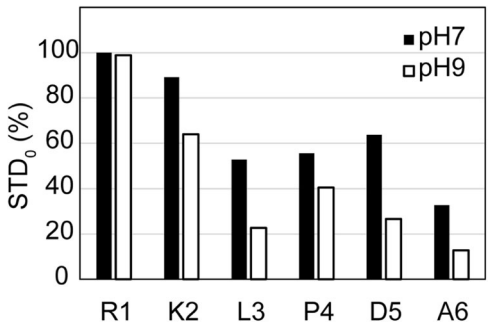

Fig. 6 Bar graph of the relative STD_0 values of a TBP/SiO_2 mixture at pH 7 (black bars) and pH 9 (white bars). The STD_0 value for the R1 Hβ proton of the TBP at pH 7 is set to 100%

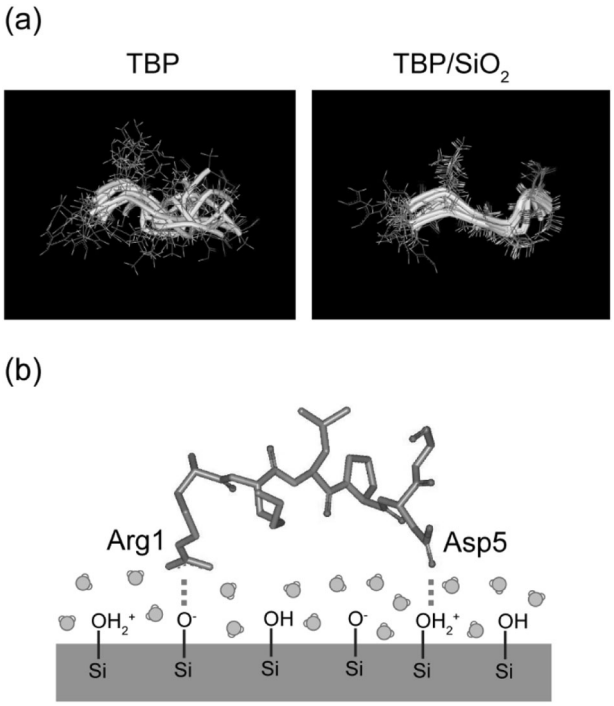

Fig. 7 **a** Overlay of the 10 best-matched model structures of the free TBP (left) and the TBP bound to a SiO_2 surface (right). The average backbone RMSDs for the free TBP and the SiO_2-bound TBP are 1.37 ± 0.34 and 0.38 ± 0.06 Å, respectively. **b** TBP/SiO_2 binding model proposed in this study. NH_2^+ in the side chain of Arg1 and COO^- in the side chain of Asp5 interact with SiO^- and $SiOH_2^+$ on the SiO_2 surface by electrostatic interaction

zeta potential means that the SiO_2 surface is more negatively charged at pH 9 than at pH 7. These results show that with an increase in pH from 7 to 9, the electrostatic interaction between the side chain group COO^- of the Asp5 and SiO_2 surface is weakened, thus resulting in a large decrease in the STD_0 values of Asp5 and the neighboring residues Pro4 and Ala6. These results provide evidence for the existence of electrostatic interactions between the COO^- group of the Asp5 residue and the protonated silanol groups on the SiO_2 surface at pH 7.

Structure of the TBP bound to SiO_2

The structure of the TBP bound to SiO_2 was investigated by NOESY measurements. The NOESY spectrum of the TBP/SiO_2 sample shows a relatively large number of negative NOE peaks, whereas the NOESY spectrum of the free TBP in the solution shows only a few positive NOE peaks. The observation of negative NOE peaks for the TBP in the spectrum of the TBP/SiO_2 sample strongly suggests that the TBP in the bound state has a specific structure. Model structures were calculated using the DYANA program with NOE peaks of 97 for the TBP/SiO_2 sample. The 10 best-matched model structures calculated based on these NOE data are overlaid in Fig. 7a with the model structures of the free TBP obtained from the ROESY measurements in the previous study for comparison. The averaged backbone root-mean-square deviations (RMSDs) are 0.38 ± 0.06 Å for the TBP bound to SiO_2 and 1.37 ± 0.34 Å for the free TBP. It seems clear from the overlaid model structures and the RMSD values that the free TBP exhibits a nearly random structure, while the TBP bound to SiO_2 has a well-restricted structure. The average main-chain dihedral angles of the model structures are (φ, ψ) = (−29°, −145°) for Lys2; (−168°, 177°) for Leu3; (−75°, 7°) for Pro4 and (97°, −12°) for Asp5. The dihedral angles for all residues except for φ of Lys2 were well-restricted and are shown in Fig. 7b.

Considering all the experimental results, we proposed a model for the binding of the TBP on the SiO_2 surface, as shown in Fig. 7b. One of the model structures from the 10 best-matched models is shown where both side chains of Arg1 and Asp5 face toward the SiO_2 surface. The rigid conformation of Pro4 may have an advantage for this model. Proline is the only amino acid that exists in the cis conformation. This finding is due to the smaller energy difference between the cis and trans states of proline compared to the other amino acids. However, the proline residues in all 10 best-matched model structures were found to be in the trans conformation with a dihedral angle ω = 180°. The NOE cross peaks were clearly observed between Leu3 Hα and Pro4 Hδ, as they are in close contact when the proline residue is in the trans conformation. Therefore, it is suggested that the Pro4 residue plays a key role in the structural rigidity. The importance of proline has been pointed out on peptides with a binding affinity to mica by Maity et al. [8] The adhesion of a mica binding peptide was significantly reduced when proline in the peptide is replaced with alanine.

The surfaces of the SiO_2 nanoparticles in aqueous solution are composed of SiOH, SiO^-, and $SiOH_2^+$ and are covered with multiple layers of water molecules. The NH_2^+ at the guanidyl group of Arg1 and the COO^- of the Asp5 side chain electrostatically interact with SiO^- and $SiOH_2^+$ on the SiO_2 surface, respectively. Moreover, the guanidyl group of Arg1 may form hydrogen bonds with Si–O^- and/or the adsorbed water molecules through its NH and NH_2 groups in the specific binding mode of the TBP to SiO_2 nanoparticles. Non-specific binding modes also accompany the proposed specific mode because the interactions are essentially electrostatic, including the interaction between the N- and C-terminal ionic groups to the silica OH^- or OH_2^+ groups, respectively. However, it appears from the point-mutation experiments that the contributions of these non-specific binding modes are relatively small in the TBP-SiO_2 system. Thus, the specific binding mode that we propose in this study is the most prevalent binding mode in this system.

The mechanism by which the TBP binds to the SiO_2 and/or TiO_2 surfaces has been suggested by several groups. Sano

et al. [12] used atomic force microscopy (AFM) to study the interaction of ferritins fused with the original 12-mer TBP and that of its point mutants with Ti and Si substrates. These authors concluded that the replacement of Arg1, Pro4, and Asp5 in the TBP with Ala resulted in substantially weak binding to both Ti and Si surfaces. Fukuta et al. [28] also investigated the binding behavior of ferritins with Ala-substituted TBPs using AFM and showed that each single positively charged amino acid (Arg1 or Lys2) anchored the mutant ferritins on the SiO_2 and TiO_x substrates. Skelton et al. [29] reported that the TBP initially recognizes the water layers on the TiO_2 surface via a pair of oppositely charged groups, Arg1 and Asp5, or Lys2 and Asp5, as studied by molecular dynamics simulations. Schneider et al. [30] also used molecular dynamics simulations and showed that Arg1 is mainly responsible for TBP anchoring to the TiO_2 and SiO_2 surfaces and that Lys2 and Asp5 contribute to the adsorption equilibrium. Okiyama et al. [31] reported that the three charged residues, Arg1, Lys2, and Asp5, are major promoters of the adhesion of the TBP to a SiO_2 surface, as studied by molecular orbital calculations. Mirau et al. [32] proposed a compact C-shaped structure for the TBP bound to the surface of SiO_2 nanoparticles, as determined by solution NMR, suggesting that electrostatic interactions between the positive charges of the Arg1 and Lys2 side chains and the negatively charged SiO_2 surface promote peptide anchoring on the surface. All these studies performed by various groups concluded that the charged TBP amino acids are primarily involved in the interaction of the TBP with SiO_2 and/or TiO_2 and that Arg1 is particularly important for adhesion. However, these studies also showed that the other charged amino acids, Lys2 and Asp5, moderately contributed to the TBP-substrate interaction. As mentioned above, Sano et al. [12] showed that only Asp5 contributed to the interaction of the TBP with SiO_2. In contrast, Schneider et al. [30] suggested that both Lys2 and Asp5 contributed to the adsorption equilibrium, and Okiyama et al. [31] reported that both Lys2 and Asp5 as well as Arg1 were major promoters of the adhesion of the TBP to a SiO_2 surface.

Our results showed that the Arg1 and Asp5 residues directly interact with the SiO_2 nanoparticle surface. On the other hand, Arg1 and Lys2 but not Asp5 directly interact with the TiO_2 nanoparticle surface, as we reported in the previous study on the TBP/TiO_2 system [23]. That is, both positively and negatively charged groups mainly interact with the SiO_2 surface, while the two positively charged groups interact with the TiO_2 surface. Our results regarding the TBP–SiO_2 interaction are consistent with the results from Sano's group [12] in which both Arg1 and Asp5 interact with the SiO_2 surface and Pro4 strengthens the binding affinity of the TBP with the SiO_2 surface. Furthermore, our results for TBP–TiO_2 support the results of Fukuta et al. [28], which show that positively charged amino acids (Arg1 and Lys2) anchored ferritin on TiO_x; however, our results are not fully consistent with those of other groups.

In conclusion, our experimental techniques and conditions allowed us to evaluate the interaction between peptides and the surface of inorganic nanoparticles in an aqueous solution. These results are useful in the development of nanoparticle/peptide composites and will aid in the design of peptide sequences bound to an inorganic nanoparticle surface.

Conclusion

In this study, we investigated the interaction of the metal oxide binding peptide TBP to SiO_2 nanoparticle surfaces using solution NMR techniques. STD NMR measurements with the selective saturation of water molecules and mutagenesis analysis of the TBP were performed to identify the TBP sites that interact with the SiO_2 surface. The results show that Arg1 and Asp5 are essential for TBP binding to SiO_2 nanoparticles and that Pro4 plays the key role in the TBP–SiO_2 interaction. The structure of the TBP bound to the SiO_2 surface was determined by using the DYANA program based on the NOESY experiments. The results indicate that the side chains of Arg1 and Asp5 face in the same direction, most likely towards the SiO_2 surface. Taking into account this result together with the pH dependent STD strength and zeta potential, a binding model for the TBP was proposed, where the guanidyl group of the Arg1 side chain and the carboxyl group of Asp5 side chain electrostatically interact with the deprotonated and protonated silanol groups on the SiO_2 surface. Notably, the binding mode proposed here for TBP/SiO_2 is certainly different from that for the TBP/TiO_2 system, as previously reported. The STD NMR experiment developed in this study provides a powerful tool for screening and identifying peptides with a specific affinity to inorganic nanoparticles.

Acknowledgements YS thanks Prof. Tetsuo Asakura of Tokyo University of Agriculture and Technology, Japan for the helpful discussions. YS acknowledges support from a JSPS Grant-in-Aid for Young Scientists (B) (16K17957).

Compliance with ethical standards

Conflict of interest The authors declare that they have no conflict of interest.

References

1. Care A, Bergquist PL, Sunna A. Solid-binding peptides: smart tools for nanobiotechnology. Trends Biotechnol. 2015;33:259–68.
2. Seker UOS, Demir HV. Material binding peptides for nanotechnology. Molecules. 2011;16:1426–51.

3. Shiba K. Exploitation of peptide motif sequences and their use in nanobiotechnology. Curr Opin Biotechnol. 2010;21:412–25.
4. Shiba K. Natural and artificial peptide motifs: their origins and the application of motif-programming. Chem Soc Rev. 2010;39:117–26.
5. Tamerler C, Sarikaya M. Molecular biomimetics: nanotechnology and bionanotechnology using genetically engineered peptides. Philos Trans R Soc A. 2009;367:1705–26.
6. Sidhu SS, Lowman HB, Cunningham BC, Wells JA. Phage display for selection of novel binding peptides. Methods Enzymol. 2000;328:333–63.
7. Scott JK, Smith GP. Searching for peptide ligands with an epitope library. Science. 1990;249:386–90.
8. Maity S, et al. Elucidating the mechanism of interaction between peptides and inorganic surfaces. Phys Chem Chem Phys. 2015;17:15305–15.
9. Puddu V, Perry CC. Interactions at the silica-peptide interface: the influence of particle size and surface functionality. Langmuir. 2014;30:227–33.
10. Emami FS, et al. Prediction of specific biomolecule adsorption on silica surfaces as a function of pH and particle size. Chem Mater. 2014;26:5725–34.
11. Patwardhan SV, et al. Chemistry of aqueous silica nanoparticle surfaces and the mechanism of selective peptide adsorption. J Am Chem Soc. 2012;134:6244–56.
12. Sano KI, Sasaki H, Shiba K. Specificity and biomineralization activities of Ti-binding peptide-1 (TBP-1). Langmuir. 2005;21:3090–5.
13. Sano KI, Shiba K. A hexapeptide motif that electrostatically binds to the surface of titanium. J Am Chem Soc. 2003;125:14234–5.
14. Yoshinari M, Kato T, Matsuzaka K, Hayakawa T, Shiba K. Prevention of biofilm formation on titanium surfaces modified with conjugated molecules comprised of antimicrobial and titanium-binding peptides. Biofouling. 2010;26:103–10.
15. Kashiwagi K, Tsuji T, Shiba K. Directional BMP-2 for functionalization of titanium surfaces. Biomaterials. 2009;30:1166–75.
16. Kokubun K, Kashiwagi K, Yoshinari M, Inoue T, Shiba K. Motif-programmed artificial extracellular matrix. Biomacromolecules. 2008;9:3098–105.
17. Sano KI, Yoshii S, Yamashita I, Shiba K. In aqua structuralization of a three-dimensional configuration using biomolecules. Nano Lett. 2007;7:3200–2.
18. Sano K, Sasaki H, Shiba K. Utilization of the pleiotropy of a peptidic aptamer to fabricate heterogeneous nanodot-containing multilayer nanostructures. J Am Chem Soc. 2006;128:1717–22.
19. Hayashi T, Sano K, Shiba K, Iwahori K, Yamashita I, Hara M. Critical amino acid residues for the specific binding of the Ti-recognizing recombinant ferritin with oxide surfaces of titanium and silicon. Langmuir. 2009;25:10901–6.
20. Mayer M, James TL. NMR-based characterization of phenothiazines as a RNA binding scaffold. J Am Chem Soc. 2004;126:4453–60.
21. Mayer M, Meyer B. Group epitope mapping by saturation transfer difference NMR to identify segments of a ligand in direct contact with a protein receptor. J Am Chem Soc. 2001;123:6108–17.
22. Mayer M, Meyer B. Characterization of ligand binding by saturation transfer difference NMR spectroscopy. Angew Chem Int Ed. 1999;38:1784–8.
23. Suzuki Y, Shindo H, Asakura T. Structure and dynamic properties of a Ti-binding peptide bound to TiO_2 nanoparticles as accessed by H-1 NMR spectroscopy. J Phys Chem B. 2016;120:4600–7.
24. Delaglio F, Grzesiek S, Vuister GW, Zhu G, Pfeifer J, Bax A. Nmrpipe—a multidimensional spectral processing system based on unix pipes. J Biomol NMR. 1995;6:277–93.
25. SPARKY3 (University of California, San Francisco).
26. Guntert P, Mumenthaler C, Wuthrich K. Torsion angle dynamics for NMR structure calculation with the new program DYANA. J Mol Biol. 1997;273:283–98.
27. Yan JL, Kline AD, Mo HP, Shapiro MJ, Zartler ER. The effect of relaxation on the epitope mapping by saturation transfer difference NMR. J Magn Reson. 2003;163:270–6.
28. Fukuta M, Zheng B, Uenuma M, Okamoto N, Uraoka Y, Yamashita I, Watanabe H. Controlled chrged amino acids of Ti-binding peptide for surfactant-free selective adsorption. Cool Surf B Biointerfaces. 2014;118:25–30.
29. Skelton AA, Liang TN, Walsh TR. Interplay of sequence, conformation, and binding at the peptide-titania interface as mediated by water. ACS Appl Mater Interfaces. 2009;1:1482–91.
30. Schneider J, Ciacchi LC. Specific material recognition by small peptides mediated by the interfacial solvent structure. J Am Chem Soc. 2012;134:2407–13.
31. Okiyama Y, Tsukamoto T, Watanabe C, Fukuzawa K, Tanaka S, Mochizuki Y. Modeling of peptide-silica interaction based on four-body corrected fragment molecular orbital (FMO4) calculations. Chem Phys Lett. 2013;566:25–31.
32. Mirau PA, Naik RR, Gehring P. Structure of peptides on metal oxide surfaces probed by NMR. J Am Chem Soc. 2011;133:18243–8.